Nuclear Engineering and Technology 56 (2024) 1454–1459

Contents lists available at ScienceDirect

Nuclear Engineering and Technology

journal homepage: www.elsevier.com/locate/net

Original Article

Influence of fluidelastic vibration frequency on predicting damping controlled instability using a quasi-steady model in a normal triangular tube array

Petr Eret

Department of Power System Engineering, Faculty of Mechanical Engineering, University of West Bohemia, Univerzitni 22, 306 14 Pilsen, Czech Republic

ARTICLE INFO

Keywords:
Heat exchanger tube array
Fluidelastic instability
Quasi-steady model
Single degree of freedom tube
Fluidelastic frequency
Time delay

ABSTRACT

Researchers have applied theoretical and CFD models for years to analyze the fluidelastic instability (FEI) of tube arrays in steam generators and other heat exchangers. The accuracy of each approach has typically been evaluated using the discrepancy between the experimental critical flow velocity and the predicted value. In the best cases, the predicted critical flow velocity was within an order of magnitude comparable to the measured one. This paper revisits the quasi-steady approach for damping controlled FEI in a normal triangular array with a pitch ratio of $P/d = 1.375$. The method addresses the fluidelastic frequency at the stability threshold as an input parameter for the approach. The excellent agreement between the estimated stability thresholds and the equivalent experimental results suggests that the fluidelastic frequency must be included in the quasi-steady analysis, which requires minimal computing time and experimental data. In addition, the model allows a simple time delay analysis regarding flow convective and viscous effects.

1. Introduction

Fluidelastic instability (FEI) is the most perilous vibration excitation mechanism for steam generators and heat exchanger tube arrays in a cross-flow. It is equally important for liquid, gas and two-phase cross-flow and can be destructive in a matter of hours [1]. The response of a tube subjected to FEI is characterized by a rapid increase in vibration amplitude in the cross-flow direction at a critical flow velocity when energy is transferred from the flow to the tube. This critical flow velocity is one of the principal design criteria and is a limiting factor for power output in a nuclear steam generator during stretch-out operation [2]. Indeed, the nuclear power industry has led the way in the research of flow-induced vibration of tube bundles for several decades, and these efforts were summarized in the literature [3,4]. Despite the progress in FEI understanding, design guidelines are driven by a quasi-static model in the form of Connors' equation, and researchers still attempt to find the "correct" values of Connors' constant [5,6]. However, many deficiencies are associated with Connors' equation, and better design rules must be sought [7].

FEI is predominantly geometry-dependent, and there are differences in the dynamic behaviour of various tube arrays. The ratio of the centre-to-centre distance between tubes to tube diameter P/d is typically 1.25 to 2.00. Two distinct mechanisms have been recognized over the years: a fluidelastic stiffness mechanism associated with the fluidelastic coupling of adjacent tubes with at least two degrees of freedom and a negative fluid damping mechanism for a system with a single degree of freedom (sdof) [8,9]. Two mechanisms generally coexist and overlap over different ranges of mass-damping parameters ($m\delta/\rho d^2$) [10]. Many researchers have used a single flexible tube in the middle of a rigid array to investigate FEI [11–13]. The concept of testing using a single flexible tube is based on the experimental observations that, in some cases, a single flexible tube placed in a rigid tube array undergoes FEI at the same critical flow velocity as a fully flexible tube array [14]. While this approach has some limitations, it has substantial benefits for developing a clearer insight into the FEI mechanism [11,15]. A sdof tube, free to oscillate in a cross-flow, is a weakly nonlinear system with a crucial effect of nonlinear damping on limit cycle oscillations in the post-stable behaviour [13,16]. Sdof fluidelastic systems are usually linearized and require minimum empirical inputs to investigate the stability threshold [10,17–19]. Probably the best models are based on the unsteady fluid dynamic force measurements, where the dynamic character of FEI is fully captured [20,21]. Unfortunately, as generally accepted, this is done at the expense of an extensive experimental campaign, which makes these approaches, which are otherwise accurate, impractical as a design tool for various tube array configurations. In contrast, CFD analysis shows considerable promise as a prediction

E-mail address: petreret@fst.zcu.cz.

https://doi.org/10.1016/j.net.2023.11.049
Received 11 April 2023; Received in revised form 30 October 2023; Accepted 28 November 2023
Available online 1 December 2023

Nomenclature

Symbols

δ	Logarithmic decrement
$\frac{m\delta}{\rho d^2}$	Mass-damping parameter (ratio)
j	Imaginary unit
μ	Dimensionless parameter associated with time delay
ν	Kinematic viscosity
ω	Frequency in rad/s
ρ	Flow density
τ	Time delay
a	Ratio of gap flow velocity to free stream flow velocity
A, B, C, D	Calculation parameters
b	Mechanical damping coefficient
C_L	Static lift coefficient
C_D	Static drag coefficient
d	Tube diameter
f	Frequency in Hz
F_y	Fluidelastic force in y-direction
k	Mechanical stiffness coefficient
L	Characteristic length scale for viscous effects
l	Tube length
m	Mass of tube per unit length
P	Pitch separation between tubes
Re	Reynolds number $Re = \frac{Ud}{\nu}$
t	Time
U	Flow velocity
Y	Displacement amplitude
y	Tube displacement

Subscripts

0	Equilibrium position
∞	Free stream
cr	Critical
g	Gap
N	Natural
p	Predicted
T	Total

tool, but in some cases, it still needs to be capable of giving accurate predictions [22].

This study revisits the quasi-steady model, a theory of FEI of a sdof tube that assumes an essential constant time delay between tube displacement and the fluidelastic force generated thereby [18]. Several models and explanations of the origin of the time delay exist [10,14,17–19,23–25], and the current model estimates the time delay based on available experimental data. Even though the quasi-steady model with constant time delay is a simplified approach, it gives qualitatively correct predictions of the critical flow velocities [11,26]; therefore, some improvement of the approach is possible. The simple threshold of instability presented in [10] is insensitive to the frequency of oscillation in the fluid medium concerned — something that has perplexed researchers in the past [4]. The present technique uses the oscillation frequency of the tube in the fluid at the stability threshold as an input parameter.

2. Mathematical background

All tubes are considered rigid except the central one, which is also rigid, but flexibly mounted. The equation for the motion of the tube in the y-direction (cross-flow) excited by aerodynamic force F_y may be written as Eq. (1),

$$ml\ddot{y} + b\dot{y} + ky = F_y \tag{1}$$

where l is the length of the tube of mass m per unit length, b and k are the effective mechanical damping and stiffness of the tube, respectively. According to the quasi-steady theory, the aerodynamic forces acting on the oscillating tube are approximately the same as the aerostatic forces at each point of the oscillation cycle. This approach applies to most cases of instability of tube arrays in an air cross-flow, where fluid inertia can be neglected [27]. A time delay τ exists between the tube displacement y and the aerodynamic forces generated thereby [10,18]. The time delay τ is artificially inserted to force F_y and applied only to the position-dependent term of the fluid force as expressed by Eq. (2),

$$F_y = \frac{1}{2}\rho U^2 ld\left[e^{-j\omega\tau}\left(\frac{\partial C_L}{\partial y}\right)y - C_{D_0}\left(\frac{\dot{y}}{U}\right)\right] \tag{2}$$

where U is the local oncoming flow velocity (usually gap flow velocity), d is the tube diameter, ρ is the flow density, ω is the tube frequency in rad/s, C_{D_0} is the static drag coefficient about the equilibrium position and $\partial C_L/\partial y$ is the static lift coefficient differentiation in the y-direction. Similarly to the original study, C_{D_0} and $\partial C_L/\partial y$ are not Reynolds number (Re) functions due to a lack of experimental data [18].

Eqs. (1) and (2) are combined and rewritten as Eq. (3) with ω_N as the natural frequency of the oscillating tube and δ as the logarithmic decrement.

$$\begin{aligned}\ddot{y} &+ \left[\left(\frac{\delta}{\pi}\right)\omega_N + \frac{1}{2}\left(\frac{\rho U d}{m}\right)C_{D_0}\right]\dot{y} \\ &+ \left[\omega_N^2 - \frac{1}{2}\left(\frac{\rho U^2 d}{m}\right)\left(\frac{\partial C_L}{\partial y}\right)e^{-j\omega\tau}\right]y = 0\end{aligned} \tag{3}$$

For harmonic oscillations, $y = Ye^{j\omega t}$, the total damping b_T is defined by the following expression in Eq. (4).

$$\begin{aligned}b_T = &\left(\frac{\delta}{\pi}\right)\omega_N\omega + \frac{1}{2}\left(\frac{\rho U d}{m}\right)C_{D_0}\omega \\ &+ \frac{1}{2}\left(\frac{\rho U^2 d}{m}\right)\left(\frac{\partial C_L}{\partial y}\right)\sin(\omega\tau)\end{aligned} \tag{4}$$

At the instability threshold, when the flow velocity is critical, $U = U_{cr}$ (also $\omega = \omega_{cr}$), the total damping of the fluidelastic system is zero, hence the instability is associated with $b_T = 0$. Moreover, the remainder of Eq. (3) represents a coupling between the natural frequency of the tube ω_N (no flow) and the tube frequency ω_{cr} at the critical flow velocity U_{cr} as given by Eq. (5).

$$-\omega_{cr}^2 + \omega_N^2 - \frac{1}{2}\left(\frac{\rho U_{cr}^2 d}{m}\right)\left(\frac{\partial C_L}{\partial y}\right)\cos(\omega_{cr}\tau) = 0 \tag{5}$$

Eqs. (4) and (5) can be simplified as Eq. (6),

$$\begin{aligned}U_{cr}^2\sin(\omega_{cr}\tau) + \frac{B}{A}U_{cr} + \frac{C}{A} &= 0 \\ U_{cr}^2\cos(\omega_{cr}\tau) + \frac{D}{A} &= 0\end{aligned} \tag{6}$$

where $A = \frac{1}{2}\left(\frac{\rho d}{m}\right)\left(\frac{\partial C_L}{\partial y}\right)$, $B = \frac{1}{2}\left(\frac{\rho d}{m}\right)C_{D_0}\omega_{cr}$, $C = \frac{\delta}{\pi}\omega_N\omega_{cr}$ and $D = \omega_{cr}^2 - \omega_N^2$.

Eq. (6) can be solved for two unknown variables U_{cr} and τ, which are evaluated numerically, provided ω_N and ω_{cr} are known. In this approach, the oscillation frequency at the instability threshold in the fluid concerned is included in the calculation. The objective is not to determine the vibration frequency at the critical flow velocity but to assess the effect of this vibration frequency on the critical flow velocity estimate. In addition, fluid force coefficients and critical flow velocities are ideally measured on the same wind tunnel and in the same

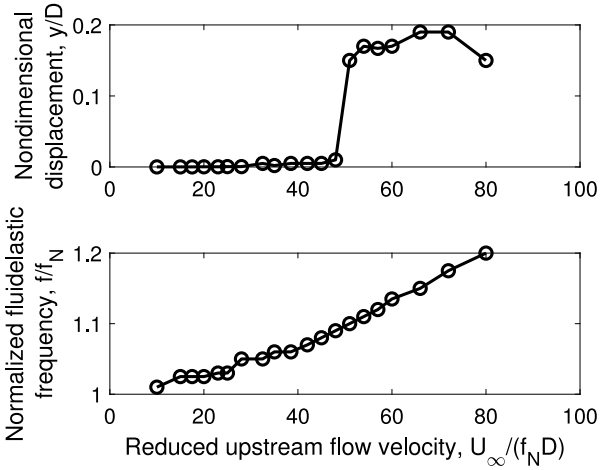

Fig. 1. Cross-flow vibratory response of the flexible tube in row 4 for $m/\rho d^2 = 2370$, $f_N = 5.11$ Hz and $\delta = 0.045$, (upper) Variation of the dimensionless displacement, (lower) Variation of the normalized natural frequency.
Source: Reproduced from [28].

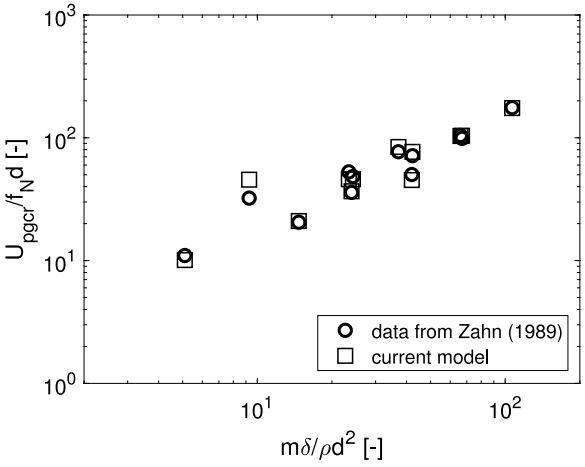

Fig. 2. Stability map for a normal triangular array with $P/d = 1.375$; current model sensitive to the fluidelastic vibration frequency.

location. The fluid force coefficients C_{D_0} and $\partial C_L/\partial y$ are the essential input parameters to the model. Different fluid force coefficients can be expected for the different tube rows as the flow takes a few tube rows to develop fully in a tube bank. The literature typically provides fluid force coefficients measured in the middle of the tube array. Few studies detail the trends of the natural frequency of a vibrating tube in a fluid.

3. Results

3.1. Tested datasets and predicted critical flow velocities

A normal triangular seven-row tube array with a pitch-to-diameter ratio of $P/d = 1.375$ ($d = 0.0254$ m) was comprehensively tested in [28], and FEI was observed predominantly in the cross-flow direction. A typical variation of the dimensionless displacement and the normalized natural frequency with the reduced upstream flow velocity is shown in Fig. 1. From these plots, the oscillation frequency at the instability threshold ω_{cr} can easily be extracted. Please note that the increasing fluidelastic frequency against the increasing flow velocity is derived only from the increasing positive linear fluid stiffness since an added mass can be neglected in the case of the air [13,16].

In the first step, 12 tests are selected due to the available frequency and stability threshold plots and the cross-flow direction of instability for row 4 in the middle of the tube array under investigation, see Table 1. In addition, the experimentally acquired fluid force coefficients related this tube array configuration are taken from the literature [19]. In particular, based on the local approach velocity, the static drag coefficient in the position of equilibrium is $C_{D_0} = 3.8/a^2$, and the static lift coefficient differentiation in the y-direction is $\partial C_L/\partial \bar{y} = -19.2/a^2$ with $a = U_g/U_\infty = (P/d)/(P/d - 1)$ and $\bar{y} = y/d$.

Experimental data are compared with the obtained results for all the mass ratios, damping parameters and frequency ratios specified in Table 1. Fig. 2 shows the predicted reduced critical flow velocities $U_{pgcr}/f_N d$ and the equivalent experimental results $U_{gcr}/f_N d = aU_{\infty cr}/f_N d$, both primarily in excellent agreement. By defining an error $\Delta = (U_{pgcr} - U_{gcr})/U_{gcr}$, the magnitude of error is higher than 10% in two cases only and less than 5% in half of the cases. The minimum error is $\Delta = -0.8\%$, and the maximum error is $\Delta = 41.3\%$; the negative sign of Δ means that the predicted values are underestimated. Excluding test number 4R3, which has the lowest damping level $\delta = 0.009$, the model is capable of delivering accurate predictions for the critical flow velocity, and the results suggest that the frequency of the oscillation of the tube in the fluid concerned at the threshold of stability is an important parameter for analyzing fluidelastic instability.

In the second step, in order to verify a systematic erroneous performance of the proposed model for low levels of damping and enhance the validation of the proposed model, experimental data across a broader range are incorporated. Data for tube rows 2, 3, 5 and 6 are hence considered and, for simplicity, the same fluid force coefficients obtained in the middle of the array are considered because the relevant experimental data are unavailable. The results for the additional 28 tests are summarized in Table 3 in Appendix. Overall, all findings obtained by the current model are far superior to the original quasi-steady approach. Only critical flow velocities for row 2 are overpredicted, which can also be attributed to the fact that this row is still at the tube array entry, and flow has no regular and repeating pattern as observed in downstream rows [28]. The tests (3R1 and 611) with low damping of $\delta = 0.008$, similar to test number 4R3, show that no systematic erroneous performance can be attributed to the proposed model for these conditions. Further analysis is performed for row 4 in the middle of the tube array, where the smallest mean error of predicted critical flow velocities was evaluated.

3.2. Comparison with the original quasi-steady model

The stability threshold for the original quasi-steady model can be estimated using Eq. (7) with $f_N = \omega_N/2\pi$ and $\mu = 1$ as a flow retardation parameter for single-phase flows [10].

$$\frac{U_{cr}}{f_N d} = \left\{ \frac{4}{-C_{D_0} - \mu d\left(\partial C_L/\partial y\right)} \right\} \frac{m\delta}{\rho d^2} \tag{7}$$

This simple model, insensitive to the fluidelastic frequency of oscillation, tends to overestimate the critical flow velocity in all test cases significantly except for the single test case 4R3 with the lowest value of damping $\delta = 0.009$ as depicted in Fig. 3. The prediction errors are tabulated in Table 1 (the last column), and the highest error $\Delta = 192\%$ can be found for the logarithmic decrement $\delta = 0.14$.

Finally, it is possible to render the current prediction model insensitive to the fluidelastic frequency of oscillation and thus make a direct comparison with the original quasi-steady model. The frequency insensitivity can be assumed by $\omega_N = \omega_{cr}$. Fig. 3 shows that the current solution is more suitable as the stability boundary, but most critical flow velocities are underestimated. Again, this finding emphasizes the necessity of including the oscillation frequency to analyze the damping controlled fluidelastic instability using the quasi-steady model.

Table 1
Selected tests from [28] for row 4; measured and predicted stability boundaries and discrepancies.

Row	Test ref.	$\frac{m}{\rho d^2}$	f_N [Hz]	δ	$\frac{m\delta}{\rho d^2}$	$\frac{\omega_{cr}}{\omega_N}$	$\frac{U_{pgcr}}{f_N d}$	$\frac{U_{gcr}}{f_N d}$	$\frac{U_{pgcr}}{f_N d}$ (Eq. (6))	Δ [%]	$\frac{U_{pgcr}}{f_N d}$ (Eq. (7))	Δ [%]
4	416	279	16.1	0.086	24	1.04	9.8	35.9	36.7	**2.1**	83.8	**133.2**
4	4R9	300	10.4	0.22	66	1.28	28.5	104.5	103.5	**−1**	230.5	**120.6**
4	410	300	17.6	0.017	5	1	3	11	10.1	**−8.2**	17.5	**58.7**
4	4R6	300	15.9	0.049	15	1.01	5.6	20.5	21	**2.3**	52.4	**155.1**
4	4R8	300	15.9	0.081	24	1.06	13.2	48.4	46	**−5**	83.8	**73.2**
4	417	300	16	0.078	23	1.06	14.4	52.8	45.9	**−13.1**	80.3	**52.1**
4	4R7	300	15.9	0.14	42	1.05	13.7	50.2	45.3	**−9.8**	146.7	**192**
4	4R3	1030	10.9	0.009	9	1.02	8.8	32.3	45.6	**41.3**	31.4	**−2.6**
4	4R2	1030	9.92	0.036	37	1.06	21	77	84.2	**9.4**	129.2	**67.8**
4	4R4	1030	11.2	0.041	42	1.05	19.5	71.5	76.8	**7.4**	146.7	**105.1**
4	4R5	1030	11.1	0.065	67	1.09	27	99	103.9	**4.9**	234	**136.3**
4	415	2370	5.11	0.045	107	1.11	48	176.0	174.6	**−0.8**	373.7	**112.3**

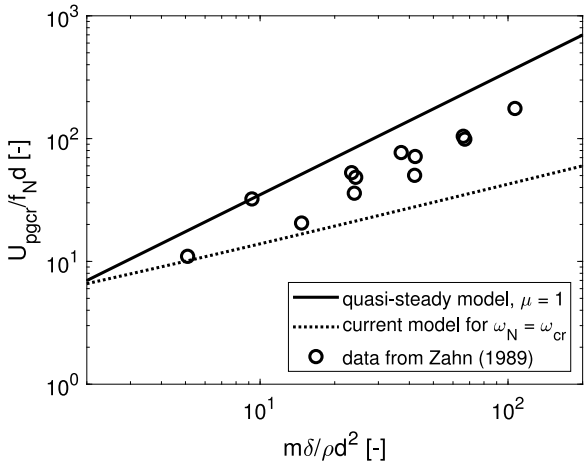

Fig. 3. Stability map for a normal triangular array with $P/d = 1.375$; current model insensitive to the fluidelastic vibration frequency.

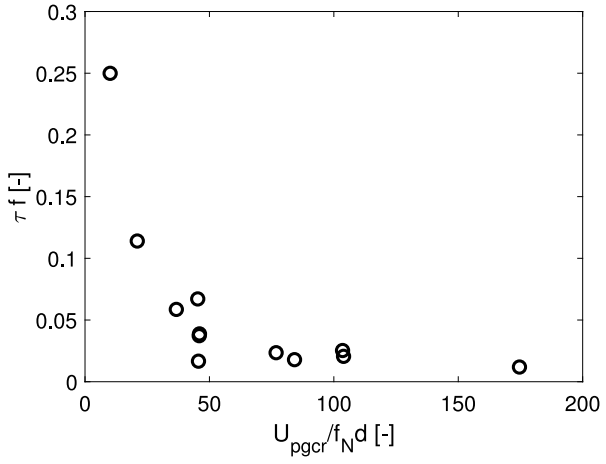

Fig. 4. Dimensionless time delay against the predicted reduced local critical flow velocity.

Table 2
Selected tests from [28], calculated time delays, dimensionless parameters of flow convective and viscous effects.

Test ref.	τ [s]	μ [−]	L/d [−]
416	0.0035	2.0741	0.0090
4R9	0.0019	1.9916	0.0066
410	0.0142	2.5290	0.0182
4R6	0.0071	2.3539	0.0128
4R8	0.0023	1.6954	0.0073
417	0.0022	1.6404	0.0072
4R7	0.0040	2.8779	0.0096
4R3	0.0015	0.7686	0.0060
4R2	0.0017	1.4349	0.0063
4R4	0.0020	1.7439	0.0069
4R5	0.0017	2.0077	0.0064
415	0.0021	1.9102	0.0071
Mean	–	1.919	–

3.3. A time delay analysis

Time delay estimations are available using Eq. (6) and summarized in Table 2 for all the twelve test cases. For simple interpretation, the time delay τ is nondimensionalized by multiplication with the associated fluidelastic frequency and plotted against the predicted reduced local critical flow velocity. The data trend in Fig. 4 means that the time delay is inversely proportional to flow velocity. A similar behaviour was observed in an experimental quantification of the time delay [29], and supports the proposition that the delay effect is due to some convection process.

The estimated time delay values can be analyzed using flow convective and viscous effects. A characteristic time scale of flow convective effects is expressed by Eq. (8),

$$\tau = \mu \frac{d}{U_g} \tag{8}$$

where μ is the dimensionless parameter and d/U_g is the time necessary for the fluid to travel a distance equal to one tube diameter. This parameter is explained by the flow retardation effect (i.e. viscous fluid slows down as it nears the cylinder producing a time delay between the cylinder displacement and the resultant change in the fluid forces) and has a value of $\mu = 1$ and $\mathcal{O}(1)$ [10,11]. Table 2 shows the parameter μ calculated using the time delay estimated by the current method. The estimates are reasonably consistent, and the mean value $\mu = 1.919$ is reconsidered for the stability threshold prediction using Eq. (7). Fig. 5 shows the significant improvement of the stability map. It can be concluded that the assumed value of $\mu = 1$ was low; however, the idea of the effect of flow retardation on fluid dynamics was sensible.

Similarly, a characteristic time scale of flow viscous effects to travel a distance L is expressed by Eq. (9) [30]. Considering kinematic viscosity of air $\nu = 1.5 * 10^{-5}$ m^2/s (for typical laboratory conditions at 20 °C and $\rho = 1.2$ kg/m^3 in [28]), the characteristic length scale for viscous effects L can be evaluated from the estimated time delays and nondimensionalized using the tube diameter d, see Table 2.

$$\tau = \frac{L^2}{\nu} \tag{9}$$

Fig. 6 depicts the dimensionless distance L/d against the predicted reduced local critical flow velocity. The values are significantly lower than one, and this implies that the characteristic length L could be associated with a boundary layer thickness, which is usually very small compared with d, and thus the time delay can be connected with viscous effects in the boundary layer rather than in a wake.

Table 3
Selected tests from [28] for row 2, 3, 5 and 6; measured and predicted stability boundaries and discrepancies.

Row	Test ref.	$\frac{m}{\rho d^2}$	f_N [Hz]	δ	$\frac{m\delta}{\rho d^2}$	$\frac{\omega_{cr}}{\omega_N}$	$\frac{U_{pgcr}}{f_N d}$	$\frac{U_{gcr}}{f_N d}$	$\frac{U_{pgcr}}{f_N d}$ (Eq. (6))	Δ [%]	$\frac{U_{pgcr}}{f_N d}$ (Eq. (7))	Δ [%]
2	2R2	300	10.3	0.098	29.4	≈1	6.1	22.4	23.4	**4.6**	101.3	**352.8**
2	2R3	300	9.87	0.55	165.0	1.12	14.2	52.1	73.4	**41.0**	576.2	**1006.6**
2	2R5	2370	7.21	0.008	19.0	1.005	6.2	22.7	37.0	**62.8**	66.3	**191.9**
2	2R4	2370	7.31	0.087	206.2	1.034	19.3	70.8	99.3	**40.3**	719.4	**916.5**
2	2R6	2370	7.31	0.29	687.3	1.15	37	135.7	211.1	**55.6**	2399.0	**1668.3**
3	3R7	300	11.1	0.087	26.1	1.005	8	29.3	22.7	**−22.6**	90.8	**209.5**
3	3R9	300	10.4	0.34	102.0	1.17	18.3	67.1	80.7	**20.3**	356.2	**430.8**
3	3R8	300	10.9	0.95	285.0	1.375	29	106.3	128.0	**20.4**	995.2	**836.0**
3	3R6	2370	4.67	0.15	355.5	1.16	47	172.3	214.3	**24.4**	1243.2	**621.4**
3	3R1	2370	7.19	0.008	19.0	1.005	10	36.7	37.0	**0.9**	66.3	**81.0**
3	3R5	2370	7.24	0.013	30.8	1.01	13	47.7	52.0	**9.1**	108.3	**127.1**
3	3R3	2370	7.16	0.041	97.2	1.03	20	73.3	90.5	**23.4**	338.7	**361.9**
3	3R2	2370	7.21	0.11	260.7	1.1	41	150.3	167.4	**11.4**	911.4	**506.3**
5	5R2	300	10.4	0.2	60.0	1.18	24.5	89.8	81.6	**−9.2**	209.5	**133.2**
5	5R5	300	10.5	0.21	63.0	1.18	25.8	94.6	81.6	**−13.7**	220.0	**132.6**
5	5R1	300	17.2	0.015	4.5	≈1	3	11.0	9.5	**−13.6**	17.5	**58.7**
5	5R3	300	16.4	0.047	14.1	1.008	5.3	19.4	19.6	**0.9**	48.9	**151.6**
5	5R4	300	16.0	0.086	25.8	1.06	13.7	50.2	46.0	**−8.4**	90.8	**80.7**
5	5R7	2370	5.26	0.042	99.5	1.07	38	139.3	138.2	**−0.8**	349.2	**150.6**
5	5R8	2370	6.04	0.14	331.8	1.1	51	187.0	168.3	**−10.0**	1159.4	**520.0**
5	5R9	2370	7.19	0.011	26.1	1.11	48	176.0	174.4	**−0.9**	90.8	**−48.40**
6	6R5	300	16.7	0.013	3.9	≈1	3.0	11.0	8.9	**−19.1**	14.0	**27.0**
6	6R3	300	16.3	0.058	17.4	1.006	5.5	20.1	19.7	**−2.3**	59.4	**194.4**
6	6R4	300	16.2	0.085	25.5	1.05	12.8	46.9	42.2	**−10.1**	90.8	**93.5**
6	6R8	338	41.4	0.0095	3.2	1.002	2.1	7.7	10.1	**31.2**	10.5	**36.1**
6	6R9	338	41.1	0.058	19.6	1.015	6.2	22.7	26.1	**14.8**	69.8	**207.2**
6	611	2370	7.02	0.008	19.0	1.006	10	36.7	40.3	**9.9**	66.3	**81.0**
6	6R2	2370	7.02	0.047	111.4	1.15	54	198.0	205.8	**3.9**	387.6	**95.8**

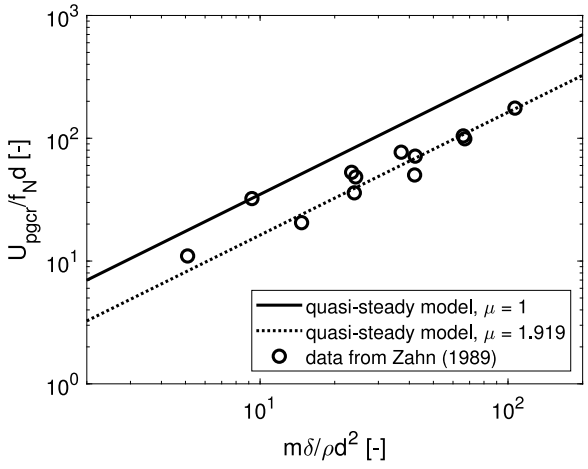

Fig. 5. Recalculation of the stability boundary based on flow convective effects.

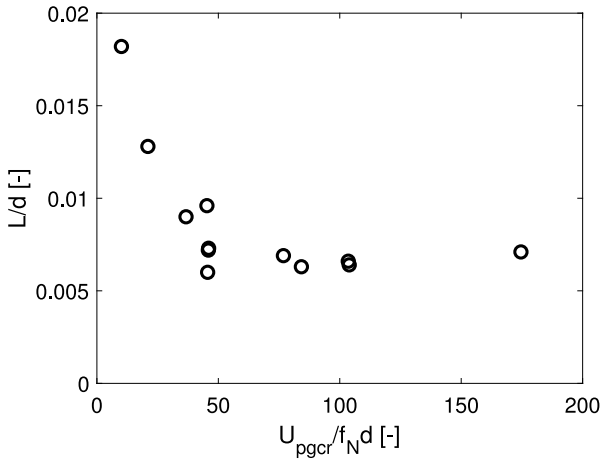

Fig. 6. Dimensionless characteristic length for viscous effects against the predicted reduced local critical flow velocity.

Moreover, the data decay in Fig. 6 seems correct as the boundary layer thickness reduces as Reynolds number increases [31]. However, a detailed analysis of the time delay origin is beyond the scope of this work.

4. Discussion

The effect of fluidelastic frequency on damping controlled fluidelastic instability prediction was assessed using a quasi-steady model. A simple model was tested using available data on a normal triangular array with $P/d = 1.375$. The predicted critical flow velocities were in excellent agreement with the experimental data, indicating the validity of this approach, meaning that the frequency of oscillation of the tube in the fluid concerned at the threshold of stability must be included when analyzing damping controlled fluidelastic instability. This finding was confirmed by directly comparing the original quasi-steady method and the current method configured to be insensitive to the oscillation frequency. In both cases, the prediction of the stability threshold was not satisfactory. In addition, the present model could deliver the magnitude of the time delay, which was investigated using flow convective and viscous effects. Although this analysis was not the main objective of the work, it was shown that convective effects in the form of flow retardation and viscous effects in the boundary layer could be associated with the time delay, and further work is required as various explanations of the time delay origin must be critically assessed.

Declaration of competing interest

The author declares that they have no known competing finan-cial interests or personal relationships that could have appeared toinfluence the work reported in this paper.

Acknowledgments

The author thanks the anonymous reviewers for their valuable comments and suggestions for corrections to improve the manuscript.

Appendix

See Table 3.

References

[1] H.G.D. Goyder, Flow-induced vibration in heat exchangers, Chem. Eng. Res. Des. 80 (3) (2002) 226–232, {UK} Heat Transfer 2001.
[2] A. Adobes, J. Pillet, F. David, M. Gaudin, Influence of steam generator tube bundle vibrations on the operating diagram of a nuclear plant during stretch out, in: ASME 2006 Pressure Vessels and Piping/ICPVT-11, Vancouver, BC, Canada, July 23-27, 2006, 2006.
[3] S.J. Price, A review of theoretical models for fluidelastic instability of cylinder arrays in cross-flow, J. Fluids Struct. 9 (1995) 463–518.
[4] M.P. Païdoussis, S.J. Price, E. de Langre, Fluid-Structure Interactions - Cross-Flow-Induced Instabilities, Cambridge University Press, 2011.
[5] X. Guangming, Z. Yong, L. Teng, T. Wei, Experimental study and analysis of design parameters for analysis of fluidelastic instability for steam generator tubing, Nucl. Eng. Technol. 55 (1) (2023) 109–118.
[6] K.-H. Lee, H.-S. Kang, D.-H. Hong, J.-I. Kim, Fluidelastic instability of a curved tube array in single phase cross flow, Nucl. Eng. Technol. 55 (3) (2023) 1118–1124.
[7] S.J. Price, An investigation on the use of Connors' equation to predict fluidelastic instability in cylinder arrays, J. Press. Vessel Technol. 123 (4) (2001) 448–453.
[8] S.S. Chen, Instability mechanisms and stability criteria of a group of circular cylinders subject to cross flow. Part I: Theory, ASME J. Vib. Acoust. Stress Reliab. Des. 105 (1983) 51–58.
[9] S.S. Chen, Instability mechanisms and stability criteria of a group of circular cylinders subject to cross flow. Part II: Numerical results and discussion, ASME J. Vib. Acoust. Stress Reliab. Des. 105 (1983) 253–260.
[10] S.J. Price, M.P. Païdoussis, An improved mathematical model for the stability of cylinder rows subject to cross-flow, J. Sound Vib. 97 (1984) 615–640.
[11] S.J. Price, M.P. Païdoussis, A single-flexible-cylinder analysis for the fluidelastic instability of an array of flexible cylinders in cross-flow, J. Fluids Eng. 108 (1986) 193–199.
[12] R. Austermann, K. Popp, Stability behaviour of a single flexible cylinder in rigid tube arrays of different geometry subjected to cross-flow, J. Fluids Struct. 9 (1995) 302–322.
[13] C. Meskell, J.A. Fitzpatrick, Investigation of nonlinear behaviour of damping controlled fluidelastic instability in a normal triangular tube array, J. Fluids Struct. 18 (2003) 573–593.
[14] J. Lever, D. Weaver, A theoretical model for fluidelastic instability in heat exchanger tube bundles, J. Press. Vessel Technol. 14 (1982) 147–158.
[15] A. Khalifa, D. Weaver, S. Ziada, A single flexible tube in a rigid array as a model for fluidelastic instability in tube bundles, J. Fluids Struct. 34 (2012) 14–32.
[16] P. Eret, C. Meskell, A practical approach to parameter identification for a lightly damped, weakly nonlinear system, J. Sound Vib. 310 (4–5) (2008) 829–844.
[17] J. Lever, D. Weaver, On the stability of heat exchanger tube bundles. Part I: modified theoretical model. Part II: numerical results and comparison with experiment, J. Sound Vib. 107 (1986) 375–410.
[18] M.P. Païdoussis, S.J. Price, The mechanisms underlying flow induced instabilities of cylinder arrays in crossflow, J. Fluid Mech. 187 (1988) 45–59.
[19] S. Granger, M.P. Païdoussis, An improvement to the quasi-steady model with application to cross-flow-induced vibration of tube arrays, J. Fluid Mech. 320 (1996) 163–184.
[20] H. Tanaka, S. Takahara, K. Ohta, Flow-induced vibration of tube array with various pitch to diameter ratios, J. Press. Vessel Technol. 104 (3) (1982) 168–174.
[21] S.S. Chen, Y. Cai, G.S. Srikantah, Fluid damping controlled instability of tubes in cross-flow, J. Sound Vib. 217 (5) (1998) 883–907.
[22] B. de Pedro Palomar, C. Meskell, Sensitivity of the damping controlled fluidelastic instability threshold to mass ratio, pitch ratio and Reynolds number in normal triangular arrays, Nucl. Eng. Des. 331 (2018) 32–40.
[23] N.-R. Kevlahan, The role of vortex wake dynamics in the flow-induced vibration of tube arrays, J. Fluids Struct. 27 (5–6) (2011) 829–837.
[24] A. Khalifa, D. Weaver, S. Ziada, Modeling of the phase lag causing fluidelastic instability in a parallel triangular tube array, J. Fluids Struct. 43 (2013) 371–384.
[25] B. Anderson, M. Hassan, A. Mohany, Modelling of fluidelastic instability in a square inline tube array including the boundary layer effect, J. Fluids Struct. 48 (2014) 362–375.
[26] C. Charreton, C. Béguin, K.R. Yu, S. Étienne, Effect of Reynolds number on the stability of a single flexible tube predicted by the quasi-steady model in tube bundles, J. Fluids Struct. 56 (2015) 107–123.
[27] S.S. Chen, Some issues concerning fluid-elastic instability of a group of circular cylinders in cross-flow, J. Press. Vessel Technol. 111 (4) (1989) 507–518.
[28] M.L. Zahn, Flow-induced vibration of a single flexible cylinder in a normal triangular array Master's thesis, McGill University, 1989.
[29] J. Mahon, C. Meskell, Estimation of the time delay associated with damping controlled fluidelastic instability in a normal triangular tube array, J. Press. Vessel Technol. 135 (3) (2013).
[30] C. Kleinstreuer, Engineering Fluid Dynamics: An Interdisciplinary Systems Approach, Cambridge University Press, 2005.
[31] H. Schlichting, Boundary Layer Theory, McGraw Hill, New York, 1979.